Investigating vaccination behavior and disease dynamics of a time-delayed two-strain epidemic model: An evolutionary approach

Md. Mamun-Ur-Rashid Khan
Interdisciplinary Graduate School of Engineering Sciences, Kyushu University

Md. Rajib Arefin
Interdisciplinary Graduate School of Engineering Sciences, Kyushu University

Tanimoto, Jun
Department of Advanced Environmental Science and Engineering, Faculty of Engineering Sciences, Kyushu University

https://doi.org/10.5109/5909084

KYUSHU UNIVERSITY

Investigating vaccination behavior and disease dynamics of a time-delayed two-strain epidemic model: An evolutionary approach

Md. Mamun-Ur-Rashid Khan[1,3*], Md. Rajib Arefin[1,3], Jun Tanimoto[1,2]

[1]Interdisciplinary Graduate School of Engineering Sciences, Kyushu University, Japan
[2]Faculty of Engineering Sciences, Kyushu University, Japan
[3]Department of Mathematics, University of Dhaka, Bangladesh
*Corresponding author email: mamun.math@du.ac.bd

Abstract: *The emergence of a new strain during a pandemic, like the present COVID-19, is a serious concern to the healthcare system. The most effective strategy to control this pandemic is vaccination. Many studies suggest that vaccine efficacy against the new strain may reduce. Additionally, the new strain's late arrival has a significant impact on the disease dynamics and vaccine coverage. Focusing on these issues, this study presents a two-strain epidemic model along with two vaccination provisions based on human behavior dynamics, in which the new strain appears with a time delay. Individuals can commit vaccination before and after being infected with strain 1 and both vaccinated and non-vaccinated individuals can be infected with strain 2. Our findings suggested that delaying the second strain increases the overall vaccination coverage and reduces the peak size of the infected individuals.*

Keywords: Behavior dynamics; Time delay; Two-strain epidemic; Vaccination

1. INTRODUCTION

Multistrain infection models are essential tools for studying and predicting infection dynamics in the presence of many active strains. Many illnesses, including human immunodeficiency virus (HIV), dengue fever, tuberculosis (TB), and even the current COVID-19, can arise when two or more strains coexist [1], [2]. For example, H1N1 flu virus infection is considered a seasonal influenza mutation, whereas COVID-19 is categorized as a novel SARS-CoV-1 strain. This mutation process can result in the emergence of new strains, especially if an effective medication has yet to be developed. In the epidemic's propagation phase, the time it takes for a new strain to arise also plays a crucial role. In the meantime, the cost of vaccination and the vaccine's efficiency against the new strain significantly influence worldwide epidemic dynamics.

Most compartmental models, which are prominent tools in epidemiology and health management systems, are frequently used to examine any epidemic process or pandemic. The SIR model, designed by Kermack and Mckendrick, is the most extensively used epidemiological model [3]. It has been thoroughly explored and expanded to see a variety of hypotheses and circumstances. Simply put, this model depicts how illness travels in people from the susceptible compartment (S) to the infectious compartment (I) and then to the recovered compartment (R), where people build immunity to reinfection [4], [5]. Exposed (E), quarantine (Q), hospitalized (H), and asymptomatic (A) compartments may be used in some epidemics to adequately examine disease dynamics [4], [6]–[9]. Investigation of control and mitigation measures, such as vaccination, modeling of vector-borne diseases, and the effect of birth and death dynamics is an additional application of compartmental models in epidemiology. Misinformation dissemination, corruption, and resource misuse are factors that might be examined in SIR dynamics. However, most of these models focus on the evolution of the illness instead of the individual's behavioral response to the situation. However, many infectious diseases control approaches rely on human and organizational decision-making. In this context, the new field of behavioral epidemiology that incorporates psychology and game theory into epidemiology attracted significant attention. Individual behavior, rather than a static role, is considered in the behavioral epidemiology [10]–[12]. This is a perfect environment for sociophysics, a novel science that blends statistical physics and evolutionary game theory (EGT) to better understand human behavior [13]–[15]. Bauch combined the SIR model with EGT to study the vaccine decision-making dynamics in a novel approach. Any individual can choose their immunization based on disease dynamics, vaccination cost, and vaccine effectiveness. This later evolved into the "vaccination game" concept [16].

In this study, we propose a two-strain epidemic model in which the first strain is active from the start of the disease and the second strain emerges after a while. People can be vaccinated in one of two ways: before they become infected with strain 1 or after recovering from it. The new strain can infect vaccinated and unvaccinated individuals. When people's preferred alternatives are to take a vaccination or not, as well as when to take a vaccine, the behavior model gives a framework for describing individual behavior. We also demonstrated the impact of the new strain's introduction on disease dynamics and individual vaccination behavior, as well as the total vaccine coverage considering the time delay.

2. MODEL DESCRIPTION

2.1 Epidemiological model

We propose a nine-compartmental two-strain epidemiological model based on the SVIR (susceptible, vaccinated, infected, recovered) dynamics. We also introduce two behaviors: preinfection and postinfection vaccinations of individuals. Figure 1 shows the schematic of the proposed model. The formulation of the model is given as follows:
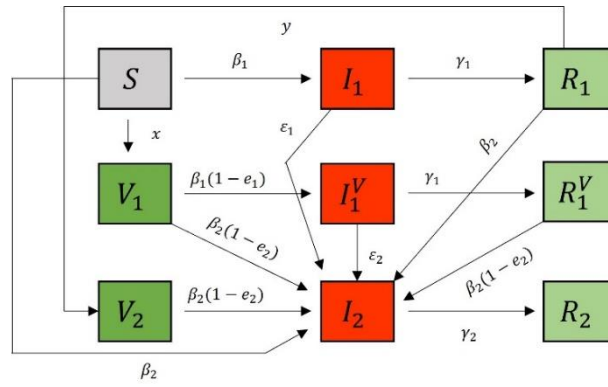
Fig. 1. Schematic of the proposed model.

$$\dot{S} = -xS - \beta_1 S(I_1 + I_1^V) - \beta_2 SI_2 H, \tag{1}$$

$$\dot{V}_1 = xS - \beta_1(1 - e_1)(I_1 + I_1^V)V_1 - \beta_2(1 - e_2)I_2 HV_1, \tag{2}$$

$$\dot{V}_2 = yR_1 - \beta_2(1 - e_2)I_2 HV_2, \tag{3}$$

$$\dot{I}_1 = \beta_1 S(I_1 + I_1^V) - \gamma_1 I_1 - \varepsilon_1 HI_1, \tag{4}$$

$$\dot{I}_1^V = \beta_1(1 - e_1)(I_1 + I_1^V)V_1 - \gamma_1 I_1^V - \varepsilon_2 HI_1^V, \tag{5}$$

$$\dot{I}_2 = \beta_2 SI_2 H + \beta_2(1 - e_2)I_2 HV_1 + \beta_2(1 - e_2)I_2 HV_2 + \varepsilon_1 I_1 + \varepsilon_2 I_1^V + \beta_2 R_1 I_2 H + \beta_2(1 - e_2)R_1^V I_2 H - \gamma_2 I_2 H, \tag{6}$$

$$\dot{R}_1 = \gamma_1 I_1 - yR_1 - \beta_2 R_1 I_2 H, \tag{7}$$

$$\dot{R}_1^V = \gamma_1 I_1^V - \beta_2(1 - e_2)R_1^V I_2 H, \tag{8}$$

$$\dot{R}_2 = \gamma_2 I_2 H, \tag{9}$$

$$H(t - T) = \begin{cases} 0, t < T \\ 1, t \geq T \end{cases} \tag{10}$$

T = time delay of the appearance of strain 2,

$$S(t) + V_1(t) + V_2(t) + I_1(t) + I_1^V(t) + I_2(t) + R_1(t) + R_1^V(t) + R_2(t) = 1, \tag{11}$$

where $S, V_1, V_2, I_1, I_1^V, I_2, R_1, R_1^V$, and R_2 are the fractions of individuals of susceptible, preinfection vaccinated, postinfection vaccinated, nonvaccinated and infected with strain 1, vaccinated and infected with strain 1, infected with strain 2, nonvaccinated and recovered from strain 1, vaccinated and recovered from strain 1, and recovered from strain 2, respectively. The Heaviside function $H(t - T)$ is used to control the time delay of the appearance of strain 2. β_1 and β_2 are the transmission rates of strain 1 and strain 2 respectively. We consider $\beta_1 < \beta_2$ because the new strain is highly transmissible. We also demonstrate the dynamics for the opposite scenario. γ_1 and γ_2 are the recovery rates from strain 1 and strain 2 respectively. Additionally, we consider $\gamma_1 > \gamma_2$, i.e., the recovery time for strain 2 is higher. e_1 and e_2 are the vaccine efficacy values to strain 1 and strain 2, respectively. We considered the fixed efficacy of the vaccine for strain 1 and strain 2 in this study where $e_1 > e_2$, but we vary the efficacy for the new strain to demonstrate the vaccination behavior and the social dilemma in the extension of this study. ε_1 and ε_2 are the mutation rates from nonvaccinated strain 1 and vaccinated strain 1 to strain 2, respectively. We have considered a very low mutation rate from strain 1 to strain 2. T represents the time delay of the emergence of strain 2. Table 1 presents all parameters and their meaning.

2.2 Behavior model
We introduce the concept of the behavior model [11], [12], which accounts for the time-varying flux from susceptible (S) to preinfection vaccination (V_1) denoted by x and from the infected but recovered from strain 1 (R_1) to postinfection vaccination (V_2) denoted by y. We define the following two dynamical equations:

$$\dot{x} = t_x x (1 - x)\{c_i (m_1 I_1 + m_1 I_1^V + m_2 I_2 H) - k c\}, \tag{12}$$

$$\dot{y} = t_y y (1 - y)\{c_i m_2 I_2 H - k c\}, \tag{13}$$

Table 1. Model parameters and their description

Parameters	Description	Parameters	Description
β_1	Disease transmission rate of strain 1	t_x	Inertial effect on preinfection vaccination
β_2	Disease transmission rate of strain 2	t_y	Inertial effect on postinfection vaccination
e_1	Efficacy of the vaccine to strain 1	m_1	Severity effect of strain 1
e_2	Efficacy of the vaccine to strain 2	m_2	Severity effect of strain 2
γ_1	The recovery rate from strain 1	c_i	Disease cost
γ_2	The recovery rate from strain 2	c	Vaccination cost
ε_1	Mutation rate from strain 1 to strain 2 for nonvaccinated	k	Relative sensitivity due to the cost of vaccination
ε_2	Mutation rate from strain 1 to strain 2 for vaccinated		

where t_x and t_y are the inertial effects for the rate of the vaccinations; c_i and c are the disease cost and vaccination cost, respectively; m_1 and m_2 are the severity effects of strain 1 and 2, respectively; and k is the relative sensitivity to taking the vaccination due to its cost. We have considered $c_i = 1.0$ throughout the study.

Most earlier models included the total number of infected people at any given time, the cost of the disease, and the cost of vaccination when calculating the dynamics of vaccines. The severity effect m_1, m_2 of the strains are considered in our study with the other parameters. The new strain frequently appears to be more severe and highly transmissible in most cases, such as the current COVID-19. To assess the dynamics of vaccination, the severity effect is also a crucial parameter. For the preinfection vaccination, we considered all infected individuals at any given time in equation (12). However, for the postinfection vaccination, we only consider the total population of individuals infected with strain 2 in equation (13). This is because individuals who did not receive the vaccine the first time may be persuaded to do so by the emergence of a highly contagious and more severe strain.

2.3 Basic reproduction number

We calculated the basic reproduction numbers for both strains using the next-generation matrix approach [17], [18].

For this, by considering the infection equations (4–6), we have

$$\mathcal{F} = \begin{pmatrix} \beta_1 SI_1 + \beta_1 SI_1^V \\ \beta_1 V_1 (1 - e_1) I_1 + \beta_1 V_1 (1 - e_1) I_1^V \\ (\varepsilon_1 I_1 + \varepsilon_2 I_1^V + (\beta_2 S + \beta_2 (1 - e_2) V_2 + \beta_2 R_1 + \beta_2 (1 - e_2) R_1^V + \beta_2 (1 - e_2) V_1) I_2) H \end{pmatrix},$$

$$\nu = \begin{pmatrix} (\gamma_1 + \varepsilon_1 H) I_1 \\ (\gamma_1 + \varepsilon_2 H) I_1^V \\ \gamma_2 I_2 H \end{pmatrix},$$

Then, from $\mathcal{F}$ and ν, we calculate the matrices as follows:

$$F = \begin{pmatrix} \beta_1 S & \beta_1 S & 0 \\ \beta_1 V_1 (1 - e_1) & \beta_1 V_1 (1 - e_1) & 0 \\ \varepsilon_1 H & \varepsilon_2 H & (\beta_2 S + \beta_2 (1 - e_2) V_2 + \beta_2 R_1 + \beta_2 (1 - e_2) R_1^V + \beta_2 (1 - e_2) V_1) H \end{pmatrix},$$

$$V = \begin{pmatrix} \gamma_1 + \varepsilon_1 H & 0 & 0 \\ 0 & \gamma_1 + \varepsilon_2 H & 0 \\ 0 & 0 & \gamma_2 H \end{pmatrix},$$

$$V^{-1} = \begin{pmatrix} \frac{1}{\gamma_1 + \varepsilon_1 H} & 0 & 0 \\ 0 & \frac{1}{\gamma_1 + \varepsilon_2 H} & 0 \\ 0 & 0 & \frac{1}{\gamma_2 H} \end{pmatrix}.$$

Then, the next-generation matrix becomes,

$$M = FV^{-1} = \begin{pmatrix} \frac{\beta_1 S}{\gamma_1 + \varepsilon_1 H} & \frac{\beta_1 S}{\gamma_1 + \varepsilon_2 H} & 0 \\ \frac{\beta_1 V_1 (1 - e_1)}{\gamma_1 + \varepsilon_1 H} & \frac{\beta_1 V_1 (1 - e_1)}{\gamma_1 + \varepsilon_2 H} & 0 \\ \frac{\varepsilon_1 H}{\gamma_1 + \varepsilon_1 H} & \frac{\varepsilon_2 H}{\gamma_1 + \varepsilon_2 H} & \frac{(\beta_2 S + \beta_2 (1 - e_2) V_2 + \beta_2 R_1 + \beta_2 (1 - e_2) R_1^V + \beta_2 (1 - e_2) V_1) H}{\gamma_2 H} \end{pmatrix}.$$

Finally, by calculating the eigenvalues of the matrix M, we have the following expressions for the basic reproduction number of strains 1 and 2.

$$R_{o1} = \frac{\beta_1 S}{\gamma_1 + \varepsilon_1 H} + \frac{\beta_1 V_1 (1 - e_1)}{\gamma_1 + \varepsilon_2 H}, \tag{14}$$

$$R_{o2} = \frac{(\beta_2 S + \beta_2 (1 - e_2) V_2 + \beta_2 R_1 + \beta_2 (1 - e_2) R_1^V + \beta_2 (1 - e_2) V_1) H}{\gamma_2 H}, \tag{15}$$

2.4 Final epidemic size and vaccination coverage

In this model, we calculated the final epidemic size in three ways: the final epidemic size of only strain 1 ($FESOS1$), the final epidemic size of only strain 2 ($FESOS2$), and the final epidemic size of both strains ($FESBoth$). The expressions for the FESs are defined as follows [10], [19]–[21]:

$$FESOS1 = R_1(\infty) + V_2(\infty), \tag{16}$$

$$FESOS2 = \int_{t=0}^{\infty} (\beta_2 SI_2 H + \beta_2 (1 - e_2) V_1 I_2 H) \, dt, \tag{17}$$

$$FESBoth = \int_{t=0}^{\infty} (\beta_2 R_1 I_2 H + \beta_2 (1 - e_2) V_2 I_2 H + \beta_2 (1 - e_2) R_1^V I_2 H + \varepsilon_1 I_1 H + \varepsilon_2 I_1^V H) \, dt, \tag{18}$$

where the argument ∞ denotes a state of equilibrium.

The vaccination coverages for preinfection v_x and postinfection v_y and the total v_c are defined as

$$v_x = \int_{t=0}^{\infty} xS \, dt, \tag{19}$$

$$v_y = \int_{t=0}^{\infty} yR_1 \, dt, \tag{20}$$

Then,

$$v_c = v_x + v_y. \tag{21}$$

3. RESULTS AND DISCUSSION

3.1 Standard (basic) case:

Figure 2(a) shows the time series graph using the standard (basic) set of parameters for the proposed model. Tables 2 and 3 present the standard values of the parameters and the initial value for the compartments and vaccination rates, respectively. We considered that the transmission rate of strain 1 (β_1) is lower than the transmission rate of strain 2 (β_2). We also considered the efficacy of the vaccine for strain 1 (e_1) is higher than the efficacy of the vaccine for strain 2 (e_2). The mutation rates $\varepsilon_1, \varepsilon_2$ from strain 1 to strain 2 were taken quite low. In the standard case, we considered the appearance of strain 2 after $T = 60$ days after the appearance of strain 1. Figure 2(b) shows that the transmission rate of strain 2 is lower than that of strain 1 (reversing the values of β_1 and β_2), with all the remaining parameters, kept the same.
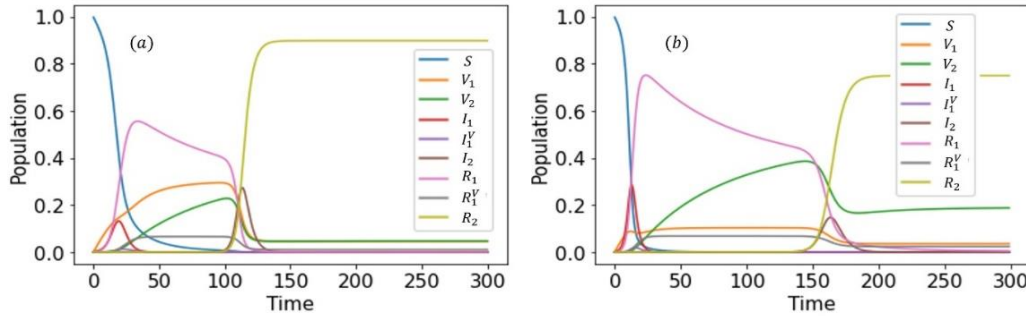

Fig. 2. Time series of the compartments for a standard case. Here, the blue line indicates the susceptible people; the orange and green lines indicate the vaccinated people before and after being infected with strain 1, respectively; red, violet, and brown indicate the infected people with strain 1 (nonvaccinated and vaccinated, respectively) and strain 2; pink and gray indicate the recovered people infected with strain 1 (nonvaccinated and vaccinated, respectively); and yellow indicates the recovered people infected with strain 2. In figure 2(a), the peak infection for strain 1 is approximately 0.15 and the peak infection for strain 2 is approximately 0.3. However, in Figure 2(b), the peak infection for strain 1 is approximately 0.3 whereas the peak infection of strain 2 is approximately 0.15. In Figure 2(a), almost 90% of the people are infected with strain 2 because the transmission rate of strain 2 is higher. However, in Figure 2(b), nearly 80% of the people are infected with strain 2 because the transmission rate of strain 2 is lower.

Table 2. Parameters and their values (standard case)

Parameter	Value	Parameter	Value
β_1	0.7	$\varepsilon_1, \varepsilon_2$	0.0001
β_2	1.0	t_x, t_y	1.0
e_1	0.7	m_1, m_2	1.0
e_2	0.5	c_i	1.0
γ_1	0.33	c	0.1
γ_2	0.25	k	0.1

Table 3. Initial values for the compartments and vaccination rate

State	At $t = 0$	State/Rate	At $t = 0$
S	0.997	I_2	0.00
V_1	0.001	R_1	0.00
V_2	0.00	R_1^V	0.00
I_1	0.001	R_2	0.00
I_1^V	0.001	x, y	0.01

3.2 Time delay effect on basic reproduction number, R_o

Figure 3 shows the time delay effect on basic reproduction numbers R_{o1} and R_{o2}. We considered four cases. The appearance of strain 2 happens after $T = 1, 60, 120, and\ 240$ days. For strain 1, the basic reproduction number always starts from the same point, approximately 2.2, and decreases with time. However, for strain 2, the starting point for the basic reproduction number decreases with time. Thus, if strain 2 appears at $T = 1$ days, i.e., almost simultaneous with strain 1, the initial value of the basic reproduction number starts from approximately 4.0 because strain 2 has a larger transmission rate. If the time delay for strain 2 is 60 days, the initial value of the basic reproduction number is approximately 3.1. Similarly, for $T = 120, 240$, the initial value of the basic reproduction number starts from 2.9 and 2.8 and decreases with the spent time.
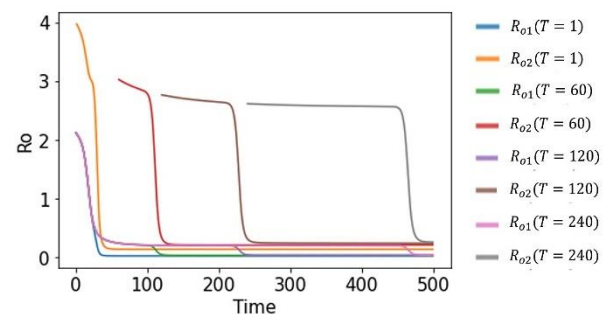

Fig. 3. Time series of basic reproduction numbers with different time delays of the appearance of strain 2. The values of the parameters are the same as those for the standard case. For strain 1, the starting points of R_{o1} are the same with different T values and they decrease with the spent time. However, the starting points of R_{o2} decrease with the delayed appearance of strain 2 and decrease with time.

3.3 Time delay effect on infection and vaccination

Figure 4 shows the infection and vaccination time series using four distinct time delays of strain 2 emergences. The total infection for strain 1 (vaccinated and

nonvaccinated) is shown in panel (a). We can see that the total infection of strain 1 is unaffected because of the time delay in the appearance of strain 2. The total infection peak is the same for $T = 1, 60, 120, 240$ (approximately 0.15). Infection for strain 2 is displayed in panel (b) showing that the infection peak decreases when the arrival of strain 2 is delayed. When $T = 1$ day, i.e., both strains are active practically concurrently from the start, the infection peak for strain 2 is the highest (approximately 0.35). However, when $T = 60, 120, 240$, the infection peaks for strain 2 are 0.28, 0.25, and 0.23, respectively. Panel (c) is made up of panels (a) and (b). As shown in these panels, the delay in the appearance of strain 2 does not affect the infection of strain 1 but it does diminish the peak size of strain 2, implying that strain 2 becomes weaker as time passes.

Preinfection, postinfection, and entire vaccination time series are illustrated in panels (d), (e), and (f). If $T = 1$, there is less time for vaccination instead of infection in panel (d). If $T = 60, 120, 240$ persons have time to be vaccinated, approximately 30% of them (vaccination peaks always occur at approximately 0.3) received their vaccination before becoming sick with any strain. In panel (e), the vaccination peaks increase as the arrival of strain 2 is delayed. After being infected with strain 1 for $T = 240$, over 35% of persons (peaking at approximately 0.35) can be vaccinated. The entire vaccination time series is presented in panel (f). We can see that delaying the appearance of strain 2 increases the possibility of postinfection vaccination and hence overall vaccination, lowering the risk of infection with strain 2, which is complementary to panels (a)−(c).
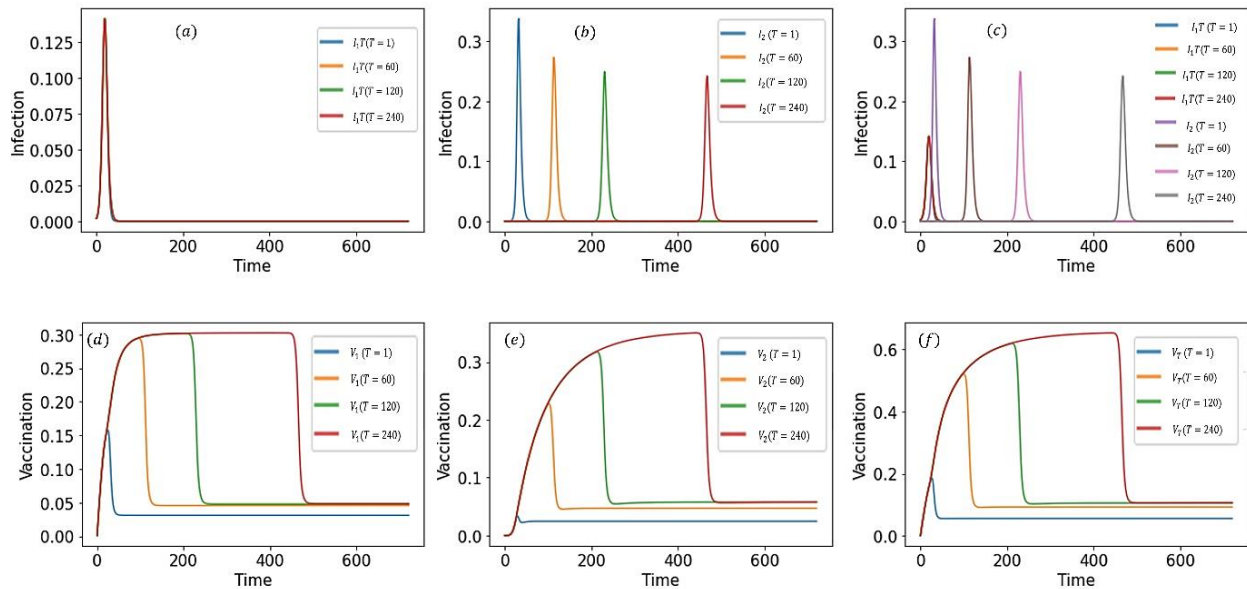

Fig. 4. Time series of infection and vaccination with a time delay of the appearance of strain 2. Panel (a) shows the total infection ($I_1 T$) due to strain 1, and panel (b) shows the total infection due to strain 2 (I_2). Both (a) and (b) show the four different time delays of the appearance of strain 2. Panel (c) is the combination of (a) and (b). Panel (d)−(f) represent the time series of preinfection vaccinated (V_1), postinfection vaccinated (V_2), and total vaccinated (V_T), respectively. Here, time delay T is taken as 1, 60, 120, 240 days and all parameters and initial values are kept the same as those of the standard case. We can observe from the panels that the time delay of the appearance can give people more chances to be vaccinated and can reduce the risk of infection from strain 2.

3.4 time delay and inertial effects on vaccination

Figure 5 shows the inertial and time delay effects on vaccination. Here, we considered three time delays $T = 60, 120, 240$, and three sets of inertial effects $(t_x, t_y) = (0.1, 0.1), (0.5, 0.5), (1.0, 1.0)$ on vaccination. For $T = 60$, panels (a)−(c) show the time series of preinfection vaccination, postinfection vaccination, and total vaccination. In panel (a), we can observe that preinfection vaccination is less with a less inertial effect and it is high with maximum inertial effect. This is obvious when the high inertial effect is active, i.e., people giving maximum effort, the preinfected vaccinees is maximum. However, the behavior of postinfection vaccination is the opposite. We can see from panel (b), that a less inertial effect gives maximum vaccines whereas a high inertial effect gives fewer vaccines. This is because, with a high inertial effect, most people take

the vaccine before they are infected with strain 1, and fewer people who can take the vaccine after being infected with strain 1 remain. Meanwhile, if fewer people take the vaccine earlier (when the less inertial effect has been considered), there will be more people remaining, those who can be infected with strain 1 and can take the vaccine to become safe from strain 2. A combination of (a) and (b) shows in panel (c), that the total vaccination looks similar, but for the less inertial effect, the peak of the total vaccination seems higher.

For $T = 120$, panels (d)−(f) are displayed. In panel (d), we can see similar behavior in preinfection vaccination time series like panel (a) which means that less inertial effect implies fewer people choose vaccination before being infected with strain 1. In panel (e), similar behavior is observed like panel (b), less inertial effect implies more people take the vaccine after being infected with strain 1. However, the infection peaks in all three cases in panel

(e) are much higher than the corresponding peaks in panel (b). Consequently, the combination of panels (d) and (e) i.e., panel (f), shows that the total vaccination peaks are also much higher than those in panel (c). This is because the time delay of the appearance of strain 2 gives much time to the people who are not vaccinated before being infected with strain 1. These people can take a vaccine when strain 2 emerges or is present.

For $T = 240$, panels (g)−(i) look almost similar to the corresponding panels (d)−(f). However, peaks in panels (h) and(i) are higher than the corresponding peaks of panels (e) and (f) because of the time delay of the appearance of strain 2. Thus, we can see that the time delay of the appearance of strain 2 can increase the chance of taking a vaccine, which can reduce the risk of infection. Additionally, a less inertial effect may help make more people vaccinated.
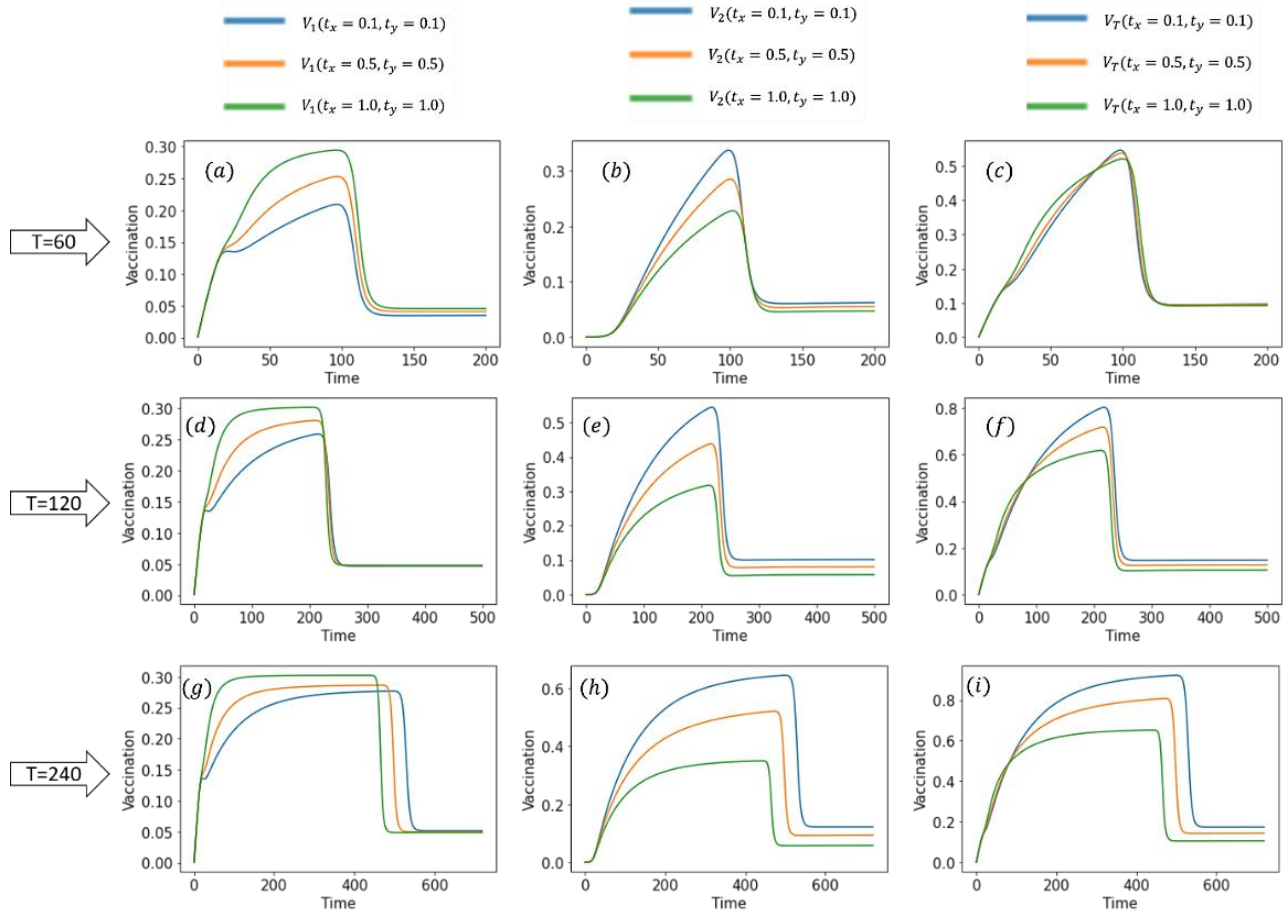

Fig. 5. Time series of preinfection vaccinated (V_1), postinfection vaccinated (V_2), and total vaccinated (V_T) people are presented with three sets of inertial effect $(t_x, t_y) = (0.1, 0.1), (0.5, 0.5), (1.0, 1.0)$ along with $T = 60, 120, 240$ days. The remaining parameters are taken as standard ones. These figures show that the time delay of the emergence of the second strain can help people be vaccinated more and less inertial effect can increase the total number of vaccinated people as a whole.

3.5 time delay and severity effects on vaccination

Figure 6 shows the severity and time delay effects of vaccination. Here, we considered three time delays $T = 60, 120, 240$, and three sets of severity effect $(m_1, m_2) = (0.1, 0.1), (0.5, 0.5), (1.0, 1.0)$ on vaccination. For $T = 60$, panels (a) − (c) show the time series of preinfection vaccination, postinfection vaccination, and total vaccination. In panel (a), we observed that the vaccination peak is highest when the severity effect is maximum. This is obvious because if the severity is higher for any strain, people must go for the vaccination as early as it is available. In panel (b), we observed almost a similar behavior with different severity effects because after being infected with strain 1, every person tries to take the vaccination to remain safer from strain 2. Panel

(c) is the combination of panels (a) and (b), which reflects that more severity implies more vaccination.

For $T = 120$, panels (d) − (f) have similar behavior corresponding to panels (a)−(c). In panel (d), the peaks of the vaccination compared to panel (a) are similar, but in panel (e), peaks are much higher than those in panel (b). This is because the time delay of the appearance of strain 2 gives more time for people to be vaccinated. Consequently, panel (f) shows that the peak of the total vaccinated people is higher than that in panel (c).

For $T = 240$, panels (g) − (i) also behave similarly compared to panels (d)−(f). However, the postinfection vaccination peak is a little higher in panels (h) and (i) than in panels (e) and (f) because of the time delay of the appearance of strain 2. Therefore, these panels show that more severe diseases can increase the chance of

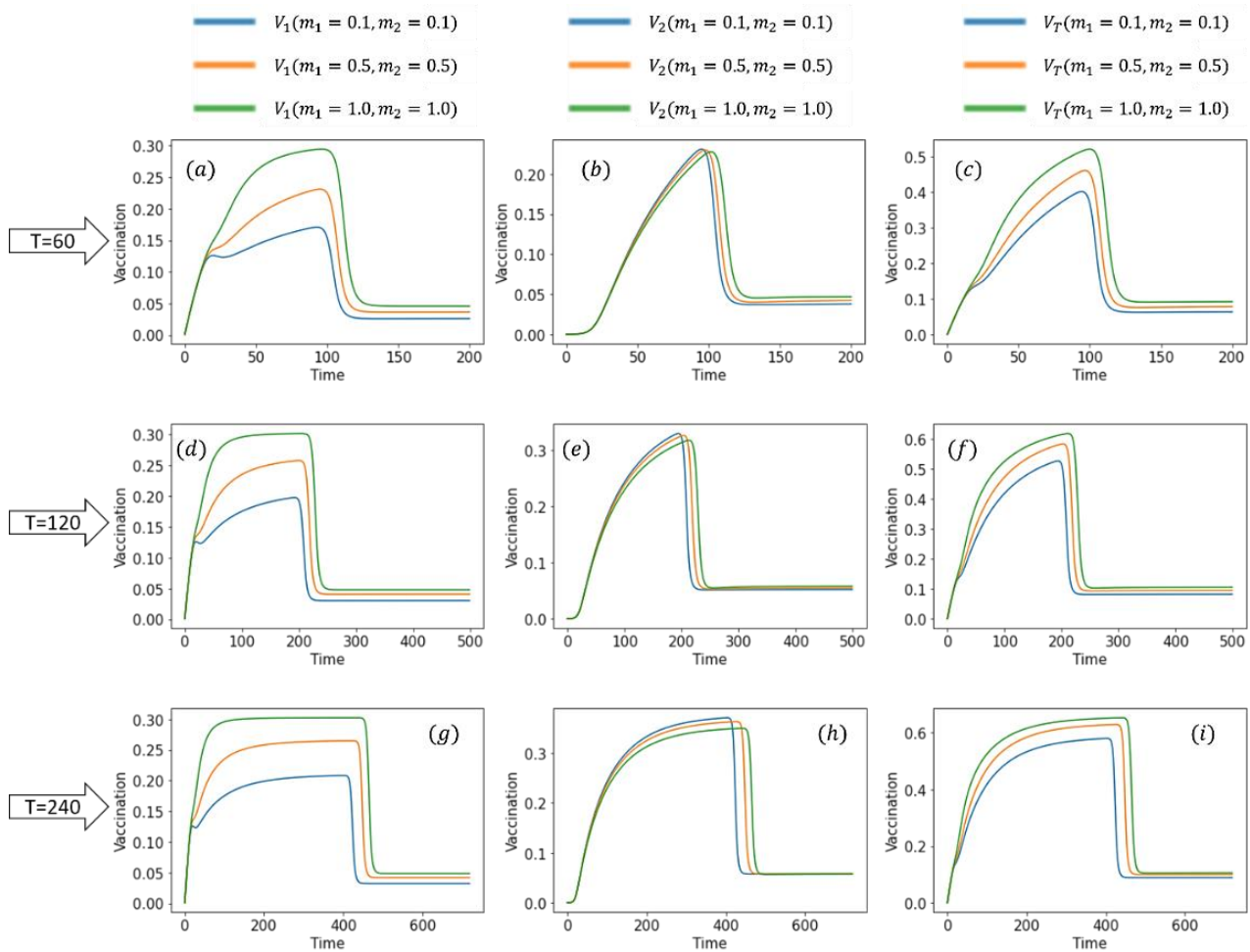vaccination and more time delay increases the chance of vaccination, which can reduce the risk of infection.

Fig. 6. Time series of preinfection vaccinated (V_1), postinfection vaccinated (V_2), and total vaccinated (V_T) people are presented with three sets of severity effects $(m_1, m_2) = (0.1, 0.1), (0.5, 0.5), (1.0, 1.0)$ along with $T = 60, 120, 240$ days. The remaining parameters are taken as standard ones. These figures show that the time delay of the emergence of a second strain can help people be vaccinated more and a higher severity effect can also increase the total number of vaccinated people.

4. CONCLUSION

The emergence of new strains creates a new challenge to the healthcare system. However, the time lag between the appearances of the resident and new strains can be substantially influential in determining the disease dynamics, especially for the second strain. Although vaccine efficacy against the new strain may reduce, its late appearance increases the possibility of higher vaccination coverage, inevitably reducing the infection peak (as well as epidemic size) concerning the new strain. This study investigated such a context by employing a two-strain epidemic model with preinfection and postinfection vaccinations. More precisely, individuals who forgo vaccination and are infected with the resident strain have the chance to be vaccinated after recovery. As vaccination is mostly voluntary, we consider behavioral dynamics to model individuals' vaccinating behavior. The decision to be vaccinated is influenced by the timing of the emergence of the new strain, its severity, transmission rate, and the cost and effectiveness of the vaccine. Most previous studies focused on stability analysis [22], competitive coexistence [23], optimal control [24], vaccination behavior [25], and disease dynamics of multistrain models.

Our primary concern was to observe the effect of vaccination and the time delay of the emergence of a new strain on controlling disease spreading. Generally, vaccination is effective in reducing the disease spreading. We also demonstrated that the time delay of the advent of a new strain could considerably reduce the corresponding basic reproduction number. Our results further suggest that the larger the time delay is, the higher the vaccination coverage, reducing the peak and the final epidemic size of the new strain.

In the extension of this work, we will investigate the social dilemma for taking vaccination of this proposed model by calculating the social efficiency deficit, which is the payoff gap between an equilibrium state and the social optimal state [26]. Additionally, we will investigate the effect of time delay on the social dilemma of taking the vaccination based on the cost and effectiveness of the vaccine.

5. REFERENCES

[1] Coronaviridae Study Group of the International Committee on Taxonomy of Viruses. The species Severe acute respiratory syndrome-related coronavirus: classifying 2019-nCoV and naming it SARS-CoV-2, Nat Microbiol 5. (2020) 536–544.

[2] S. M. Halstead, Dengue and dengue hemorrhagic fever, Handb. Zoonoses, Second Ed. Sect. B Viral Zoonoses. 11, 3, 2017, pp.89–99.

[3] W. O. Kermack, A. G. McKendrick, A contribution to the mathematical theory of epidemics, Proc. R. Soc. A Math. Phys. Eng. Sci. 115, 772 (1927) 700–721.

[4] W. Xia, S. Kundu, and S. Maitra, Dynamics of a delayed SEIQ epidemic model, Adv. Differ. Equations. 2018, 1 (2018).

[5] C. Li, J. Wang, J. Xu, Y. Rong, The Global dynamics of a SIR model considering competitions among multiple strains in patchy environments, Math. Biosci. Eng. 19 (2022) 4690–4702.

[6] M. M.U.R. Khan, M. R. Arefin, J. Tanimoto, Investigating the trade-off between self-quarantine and forced quarantine provisions to control an epidemic: An evolutionary approach, Appl. Math. Comput. 432 (2022) 127365.

[7] J. Dong, T. Li, C. Wan, X. Liu, The Analysis of a SEIRS Epidemic Model with Time Delay on Complex Networks, OALib. 04 (2017) 1–10.

[8] O. Khyar, K. Allali, Global dynamics of a multi-strain SEIR epidemic model with general incidence rates: application to COVID-19 pandemic, Nonlinear Dyn. 102 (2020) 489–509.

[9] M. Martcheva, A non-autonomous multi-strain SIS epidemic model, J. Biol. Dyn. 3 (2009) 235−251

[10] Q. Yin, Z. Wang, C. Xia, C. T. Bauch, Impact of co-evolution of negative vaccine-related information, vaccination behavior and epidemic spreading in multilayer networks, Commun. Nonlinear Sci. Numer. Simul. 109 (2022) 106312.

[11] C. T. Bauch, Imitation dynamics predict vaccinating behaviour, Proc. R. Soc. B Biol. Sci. 272 (2005) 1669–1675.

[12] C. T. Bauch and S. Bhattacharyya, Evolutionary game theory and social learning can determine how vaccine scares unfold, PLoS Comput. Biol. 8 (2012)

[13] J. Tanimoto, Sociophysics approach to epidemics. Springer, Tokyo, 2021.

[14] J. Tanimoto, Fundamentals of evolutionary game theory and its applications. Springer (Tokyo), 2015.

[15] J. Tanimoto, Evolutionary games with sociophysics: Analysis of traffic flow and epidemics. Springer, Tokyo, 2019.

[16] M. R. Arefin, T. Masaki, K. M. A. Kabir, J. Tanimoto, Interplay between cost and effectiveness in influenza vaccine uptake: A vaccination game approach, Proc. R. Soc. A Math. Phys. Eng. Sci. 475 (2019).

[17] M. Martcheva, An Introduction to Mathematical Epidemiology. Springer International Publishing, 2013.

[18] X. Z. Li, J. X. Liu, M. Martcheva, An age-structured two-strain epidemic model with super-infection, Math. Biosci. Eng. 7 (2010) 123–147.

[19] R. Tori, J. Tanimoto, A study on prosocial behavior of wearing a mask and self-quarantining to prevent the spread of diseases underpinned by evolutionary game theory, Chaos, Solitons and Fractals, 158 (2022) 112030.

[20] F.B. Agusto, I. V. Erovenko, A. Fulk, Q. Abu-Saymeh, D. Romero-Alvarez, J. Ponce, S. Sindi, O. Ortega, J. M. Saint Onge, A. Townsend Peterson, To isolate or not to isolate: the impact of changing behavior on COVID-19 transmission, BMC Public Health, 22 (2022) 1–20, 2022.

[21] M. Jusup, P. Holme, K. Kanazawa, M. Takayasu, I. Romić, Z. Wang, S. Geček, T. Lipić, B. Podobnik, L. Wang, W. Luo, T. Klanjšček, J. Fan, S. Boccaletti, M. Perc, Social physics, Phys. Rep. 948 (2022) 1−148.

[22] S. Allali, A. Amine, Stability analysis of a fractional-order two-strain epidemic model with general incidence rates, Commun. Math. Biol. Neurosci. 43 (2022).

[23] C. Li, Y. Zhang, Y. Zhou, Competitive Coexistence in a Two-Strain Epidemic Model with a Periodic Infection Rate, Discret. Dyn. Nat.Soc. 2020 (2020)

[24] E. F. Arruda, S. S. Das, C. M. Dias, D. H. Pastore, Modelling and optimal control of multi strain epidemics, with application to COVID-19, PLoS One. 16 (2021) 1–18.

[25] C. Zuo, F. Zhu, Y. Ling, Analyzing COVID-19 Vaccination Behavior Using an SEIRM/V Epidemic Model With Awareness Decay, Front. Public Heal. 10 (2022) 1–12.

[26] M. R. Arefin, K. M. A. Kabir, M. Jusup, H. Ito, J. Tanimoto, Social efficiency deficit deciphers social dilemmas, Sci. Rep. 10 (2020) 1–9.